*Transactions of the Materials Research Society of Japan* 25 [4] 1123-1126 (2000)

# Structure change in γ-TiAl induced by inert gas ion irradiation

M. Song*, K. Mitsuishi, K. Furuya, T. Tanabe and T. Noda
National Research Institute for Metals, 3-13 Sakura, Tsukuba, 305-0003 JAPAN
*Fax: 81-298-59-5054, e-mail: msong@nrim.go.jp

γ-TiAl intermetallic alloy specimens were implanted with He and Xe ions in a high-voltage transmission electron microscope (HVTEM) at room temperature. The defect formation and structure change were investigated with conventional and high-resolution transmission electron microscopy (CTEM and HRTEM). Induced defects in the He irradiated specimens are mainly planar defects and rotated domains (RDs). The planar defects have the edges parallel to {111) of the matrix and several nanometers in size. They correspond to the streaks along <111] in selected area diffraction (SAD) patterns of the ion irradiated specimens. The RDs, which are rotated 90 degree to the matrix, are formed in as-irradiated and post-irradiation annealed specimens. They are identified by the appearance of super-lattice reflection spots in SAD patterns and by image contrast in HRTEM observation as well. While a phase transformation was observed in specimens implanted with Xe ions with a much small dose than that of He ions. It is suggested that what kind of structure change takes place depends on the implanted ions, and that the sizes of the implanted ions are believed to play an important role in the phase transformation.

Key words: TiAl, Xenon, Helium, phase transformation, HRTEM

## 1. INTRODUCTION

Intermetallic TiAl alloys are being used in airplane and spaceship manufacturing because of their high strength-to-weight ratio and good resistance in temperature variation conditions [1, 2]. Potential applications in other fields are also under consideration. For example, these materials are considered as the promising candidate first wall materials for fusion reactors [3, 4]. Stability of the structure of the alloys in various conditions is a very important factor for its applications.

Irradiation effects of the TiAl alloys irradiated with energetic particles have been studied by several research groups. Dislocation loops and He bubbles were reported to be induced in TiAl alloys irradiated with electrons or He ions at 623 to 773K [4-7]. While with He ion irradiation at room temperature, planar defects and rotated domains were observed in γ-TiAl alloys [8,9]. Recently, authors reported that a phase transformation was induced in γ-TiAl alloys with Xe ion irradiation [13-15]. Irradiation effects on mechanical properties of TiAl alloys were also researched [10-12]. However, the knowledge on the mechanisms of the structure changes due to ion irradiation/implantation into γ-TiAl alloys is still very limited.

In the present work, the γ-TiAl specimens were irradiated with He and Xe ions, since the He is a kind of typical light inert gas which is a product gas in the fusion reactor circumstance and the Xe is a kind of typical heavy inert gas which is usually a product gas in nuclear reaction circumstance such as in nuclear reactors. The crystal structure change and the related mechanisms are studied. It is shown that the structure change is largely dependent on the difference in ion species and that the sizes of implanted ions plays an important role in the phase transformation.

## 2. EXPERIMENTAL

Single phased γ-TiAl alloy, with compositions (wt%) of Al 36.8 (50.81 at.), O 0.038, C 0.005, and Ti balanced, was used. Disks, 3 mm in diameter and 0.2 mm in thickness, were prepared mechanically and annealed at 1273 K (about 2/3 of the melt point) for 1 hour. The thin foil specimens were electropolished by a twin jet technique in a solution of 10% percloric acid and 90% ethanol at about 255 K.

Ion implantations were carried out at room temperature in a system consisting of a 1000 kV high voltage transmission electron microscope (HVTEM) (JEM-ARM1000), a 200 keV and a 30 keV ion implanters [16]. The energies of He and Xe ions were 15 and 50 keV, respectively. The stopping ranges of the two ions calculated with TRIM code [17] are about 102 and 25 nm, and the strugglings 50 and 6 nm, respectively, in γ-TiAl. The electron beam was switched off during ion implantation. The maximum doses of He and Xe ions were $8.6 \times 10^{20}$ and $2.6 \times 10^{20}$ ions•$m^{-2}$, respectively. The specimens are observed during and after ion implantations using a JEM-ARM1000 TEM operated at 1000 kV.

## 3. RESULTS AND DISCUSSIONS

Defect clusters became visible at a He irradiation dose of $4.7 \times 10^{19}$ ions•$m^{-2}$ and the density of the defects increased with the increasing ion dose [8]. Fig. 1a and b give a diffraction contrast (DIFC) micrograph and a corresponding selected area diffraction (SAD) pattern respectively of a specimen irradiated with He ions to a dose of $8.6 \times 10^{20}$ ions•$m^{-2}$. The specimen is observed in [011] direction of γ-TiAl crystals. Since the electron beam of the HVTEM was switched off during the irradiation, the morphology change in Fig. 1a is considered as a result of the He ion irradiation. The defects seen in Fig. 1a are mainly planar defects with edges along {111) planes as indicated by A and B

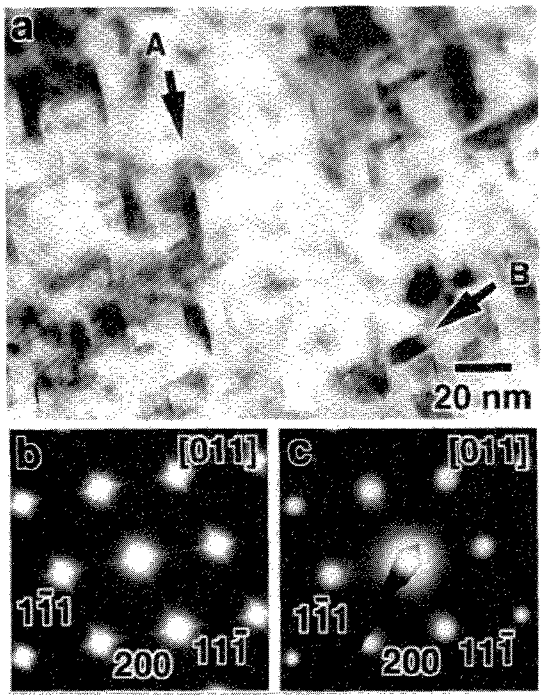

Fig. 1 A micrograph (a) in diffraction contrast (DIFC) mode and a selected area diffraction (SAD) pattern (b) of a γ-TiAl specimen irradiated with 15 keV He to a dose of 8.6 x 10$^{20}$ ions•m$^{-2}$ at room temperature.

in the figure. The width and length of the planar defects range from several nm to about 10 nm, respectively. Strong streaks in <111] directions in the SAD pattern in Fig. 1b are considered to correspond to the planar defects in the crystal. HRTEM observation reveals that the planar defects correspond to lattice structure defects in γ-TiAl crystals [8,9]. Furthermore, extra weak spots at 1/2[200] and its equivalent positions are seen in the SAD pattern, as compared with the SAD in fig. 1c of the un-irradiated specimen. These extra spots suggest that structure changes have taken place in the crystals.

γ-TiAl crystals are in an ordered L1$_0$ structure, in which Al and Ti atom layers stack alternatively along [001] direction. The unit cell is very similar to an fcc unit cell, but [110] is not equivalent to [011] and [101] crystallographically, so that a crystal direction group such as <110> and a crystal plane group such as {111} are written as <110] and {111) for expressing the difference of the L1$_0$ from an fcc structure. Diffraction pattern of the crystal along zone axis [011] or [101] is similar to that of a fcc crystal. On the other hand, extra spots due to super-lattice reflection are expected at 1/2[002] and its equivalent positions in a SAD pattern in zone axis [110]. The extra spots seen in the SAD pattern as seen in Fig. 1b are at the same positions as the super-lattice reflection of (001) of the γ-TiAl crystals when it is observed in [110] direction. This result suggests that a small part in the matrix changes its orientation from [011] to [110]. When the incident electron beam is in [011] for the matrix, it is in [110] for those orientation-changed portions so that the (001) super-lattice reflections can be observed at almost the same positions as that of 1/2[200] and its equivalent positions. Such an orientation-changed portion was noted as a rotated domain (RD), which is in a relation of 90 degrees rotation to the matrix [18-20].

Fig. 2 shows an HR micrograph, an SAD pattern of a specimen irradiated with He ions to a dose of 8.4 x 10$^{20}$ ions•m$^{-2}$ at room temperature, and calculated lattice images using a multi-slice method. The specimen is observed in [110] direction. A typical He

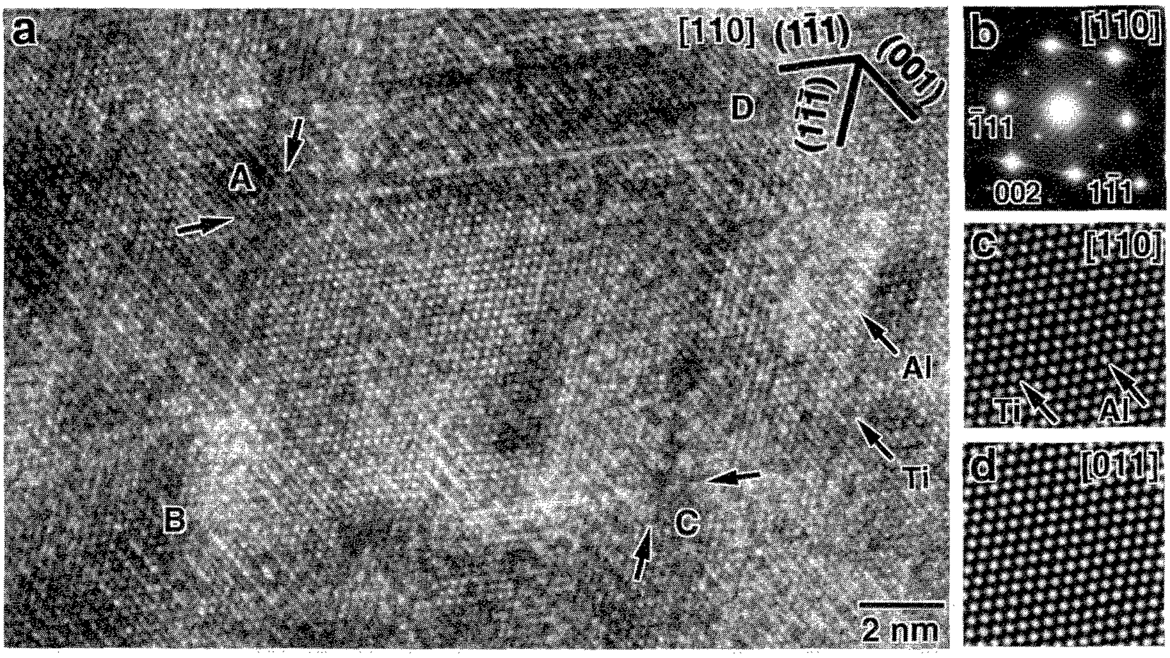

Fig. 2 Defect structure in γ-TiAl crystal irradiated with 15 keV He to a dose of 8.4 x 10$^{20}$ ions•m$^{-2}$ at room temperature. a): an HRTEM image of an RD indicated by ABCD; b): an SAD pattern; c) and d): calculated images of γ-TiAl crystals in [110] and [011] respectively with defocus of -95 nm.

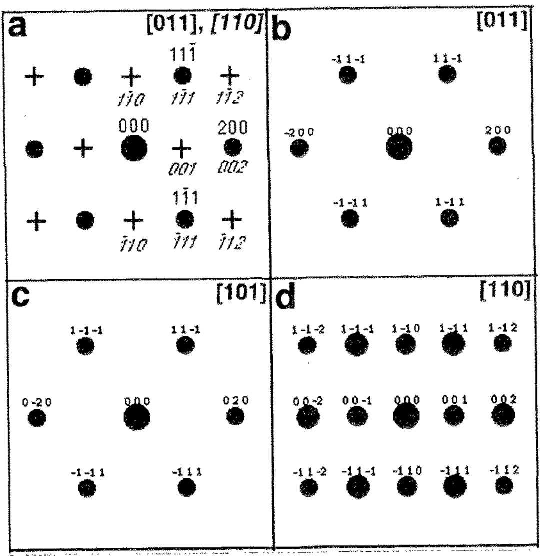

Fig. 3 Explanation of the extra spots in a [011] SAD pattern. a): a [011] SAD pattern with extra spots; b), c) and d): in [011], [101] and [110] direction respectively. Overlapping of b), c) and d) forms a).

irradiation defect structure is shown in Fig. 2a. The SAD pattern in Fig. 2b looks similar to that shown in Fig. 1b, but it is in [110]. Super-lattice fringes in space of (001) crystal face are seen in Fig. 2a. In the center part of the micrograph indicated by ABCD and arrows, a quadrilateral with a size of about 10 nanometers is seen, in which the super-lattice fringes are not seen or become weak. Fig. 2c and d show the calculated images of γ-TiAl crystals in [110] and [011], respectively. In this calculation it is assumed that 4096 waves are excited in the crystal. The imaging parameters were Cs = 2.6 mm, defocus $\Delta f = -95$ nm, specimen thickness t = 10 nm and the accelerating voltage of electron beam is 1000 kV. The lattices of Al and Ti atoms show different brightness in Fig. 2c due to the super-lattice reflection. On the other hand, the lattice fringes along (001) in Fig. 2d have the same brightness because there is no super-lattice reflection effect in this orientation. Since the areas inside and outside the quadrilateral ABCD should be observed in the same defocus, it would be concluded by comparing the image in Fig. 2a with the calculated images that the areas inside and outside the quadrilateral are in orientation of [110] and [011] respectively. The defocus corresponding to Fig. 2a are estimated as about -95 nm by comparing the figure with the calculated results. These results suggest that the quadrilateral ABCD is in [011] zone axis, i.e., an RD in the [110] matrix. This RD is considered as an irradiation induced RD in γ-TiAl, since it is typically observed in the He ion irradiated specimens.

The extra spots in SAD pattern can be explained schematically with Fig. 3. When a specimen is observed in [011] direction, the RDs in the specimen are in [101] or [110] directions. Their diffraction patterns are shown in Fig. 3b, c and d, respectively. When they exist in a selected area, the SAD pattern will be a overlapping of these three patterns, as shown in Fig. 3a. It is reasonable to think that the SAD patterns in Fig. 1b are formed in the similar way.

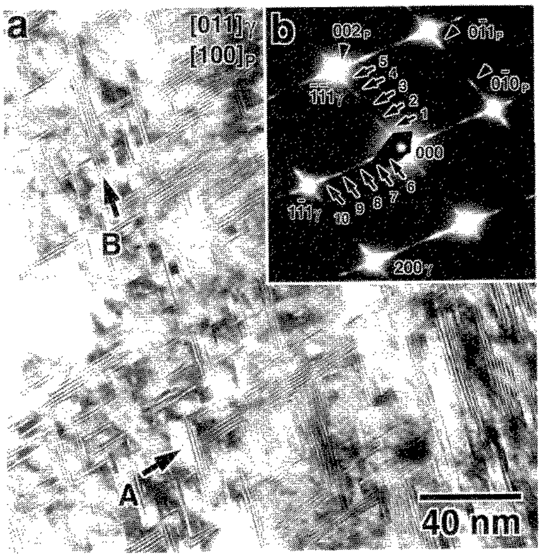

Fig. 4 A DIFC mode bright field image (a) and an SAD pattern of a γ-TiAl specimen implanted with 50 keV Xe ions at room temperature to a dose of 2.2 x $10^{18}$ ions•m$^{-2}$.

Fig. 4 shows a micrograph in DIFC mode and an SAD pattern of a specimen implanted with Xe ions to a dose of 2.2 x $10^{18}$ ions•m$^{-2}$. The specimen was observed in [011] direction of γ-TiAl phase. Planar zones were observed in fig. 4a and extra diffraction spots were observed in the SAD pattern in addition to the spots of γ-TiAl matrix in fig. 4b. The planar zones are in size of about 10 nm in width and several ten nm in length. A and B indicate two orientated defects in fig. 4a. Each of them parallels to one of the {111) of the matrix with their longer sides. Numbers 1 to 5 and 6 to 10 in fig. 4b indicate the typical extra spots in [111] and [111] directions, respectively. The extra spots in the SAD pattern are symmetrical to [002] of the γ-phase. The existence of the extra spots suggests that a second phase is induced by Xe ion implantation in the specimen. A symmetrical arrangement of the extra spots to $[002]_\gamma$ (the suffix γ means the γ-phase) reveals that the induced phase has two orientations symmetrical to $[002]_\gamma$. It is considered that the phase transformation is induced in a surface layer in a thickness of the order of projected range of the Xe ions, so that the phase transformation is observable with TEM in the thin area of the irradiated specimens.

The induced phase was identified as an Al solid solute α-Ti with parameters a = 0.284 nm and c = 0.460 nm [13-15]. The induced phases are in [100]p (the suffix p means the induced phase) direction. One set of the basic spots of the extra spots in fig. 4b is indexed in the SAD pattern. It is obvious that the phase has orientation relationships with the γ-phase of $(001)_P//\{111\}_\gamma$ and $[100]_P //<011]_\gamma$. Other extra spots are actually the second diffractions from diffraction beams of the matrix or the induced phases. For example, the second diffraction from [111]γ induces extra spot 1, and etc..

Different kinds of structure changes were observed in the present work. They are the planar defects and RDs in He irradiated specimens and the induced phase transformation in Xe implanted specimens. The development of the planar defects and the RDs is considered due to radiation damages and its recovering in crystals induced by high energetic electrons and ions, which concerns the producing and movement of point defects such as interstitials and vacancies [4-9].

It is shown that the phase transformation is dependent on the implanted/irradiated ions. Other factors may also relate to the phase transformation, such as the doses, the irradiation damages, concentrations of the implanted ions, the sizes of the implanted ions, and etc.. He ions were implanted/irradiated into specimens with much larger dose ($8.6 \times 10^{20}$ ions $m^{-2}$) than the doses of Xe ions ($2.2 \times 10^{18}$ ions $m^{-2}$), so as to He bubbles were formed [8], but no phase transformation was found. The damages in the two cases are 4.6 and 2.3 dpa, and the concentrations of the two kinds of ions are 0.149 and $3.1 \times 10^{-3}$ ppm for He and Xe ions, respectively. These facts suggest that the effects of implantation dose, damages, and concentrations of implanted ions are not significant to the phase transformation.

A possible explanation is that the sizes of the implanted ions play a role in the induced phase transformation. The radius of Xe and He ions are 0.175 and 0.100 nm, respectively, while those of Al and Ti are 0.143 and 0.147, respectively. Ions implanted into γ-TiAl alloy crystals may introduce strain in the crystals. Elastic energy in the crystals increases. The larger the ion size, the more intense the introduced strain, so that the larger the elastic energy increases. Since a Xe ion has a much larger size than a He ion, a much more intense strain level is expected to be introduced in γ-TiAl crystals with Xe ion implantation than with He ion's. The atomic density (numbers of atoms per unit volume) of the induced phase is calculated to be 0.3% larger than the γ-TiAl matrix. Therefore, the formation of the induced phase is favorable to lower down the strain level in γ-TiAl matrix, and also to decrease the elastic energy in the crystals, hence the phase transformation is much more easily to be induced in Xe ion implanted specimens than in He implanted ones.

## 4. CONCLUSIONS

γ-TiAl intermetallic alloy specimens were implanted with He and Xe ions in a high-voltage transmission electron microscope (HVTEM) at room temperature. The defect formation and structure change were investigated with conventional and high-resolution transmission electron microscopy (CTEM and HRTEM). Induced defects in the He irradiated specimens are mainly planar defects and rotated domains (RDs). The planar defects have the edges parallel to {111} of the matrix and several nanometers in size. They correspond to the streaks along <111] in selected area diffraction (SAD) patterns of the ion irradiated specimens. The RDs, which are rotated 90 degree to the matrix, are formed in as-irradiated and post-irradiation annealed specimens. They are identified by the appearance of super-lattice reflection spots in SAD patterns and by image contrast in HRTEM observation as well. While a phase transformation was observed in specimens implanted with Xe ions with a much small dose than that of He ions. It is suggested that what kind of structure change takes place depends on the implanted ions, and that the sizes of the implanted ions are believed to play an important role in the phase transformation.

## REFERENCES

1. M. Matsuo, ISIJ Int., **31**, 1212-1222 (1991).
2. F. Appel and R. Wagner, Mater. Sci. and Eng., **R22**, 187-268 (1998).
3. S. Mori, H. Miura, S. Yamazaki, T. Suzuki, A. Shimizu, Y. Seki, T. Kunugi, S. Nishino, N. Fujisawa, A. Hishinuma and M. Kikuchi, Fusion Technol., **21**, 1744-1748 (1992).
4. A. Hishinuma, J. Nuclear Mater., **239**, 267-272 (1996).
5. K. Nakata, K. Fukai, A. Hishinuma, K. Ameyama and M. Tokizane, J. Nucl. Mater., **202**, 39-46 (1993).
6. K. Nakata, K. Fukai, A. Hishinuma and K. Ameyama, J. Nucl. Mater., **240**, 221-228 (1997).
7. A. Hishinuma, K. Nakata, K. Fukai, K. Ameyama and M. Tokizane, J. Nucl. Mater., **199**, 167-171 (1993).
8. M. Song, K. Furuya, T. Tanabe and T. Noda, J. Nucl. Mater., **271&272**, 200-204 (1999).
9. M. Song, K. Furuya, T. Tanabe and T. Noda, J. Electro. Micro., **48**, 355-360 (1999).
10. E. M. Grala and J. B. McAndrew, "Mechanical properties of intermetallic compounds", Ed. by J .H. Westbrook, Wiley, New York (1960) pp. 229.
11. N. L. Petouhoff, A. J. Ardell, W. C. Oliver and B. N. Jucas, "Structural intermetallics", Ed. by R. Darolia, J. J. Lewandowski, C. T. Liu, P. L. Martin, D. B. Miracle and M. V. Nathal, The Minerals, Metals and Materials Society, USA, (1993) pp. 77.
12. A. Kohyama, T. Yamada, M. Ogawa, H. Matsui and M. Narui, "Proc. of the 2nd Japan/China sym. in materials for advanced energy systems and fission and fusion engineering", The University of Tokyo, Japan, (1994) pp. 472.
13. M. Song, K. Furuya, T. Tanabe and T. Noda, "Abstracts of the Japan institute of metals", The Japan Institute of Metals, Tokyo, (1999) pp. 283.
14. M. Song, K. Furuya, T. Tanabe and T. Noda, "Proc. of the fifty fifth annual meeting of the Japanese society of electron microscopy", The Japanese Society of Electron Microscopy, Nagoya, (1999) pp. 99.
15. M. Song, K. Furuya, T. Tanabe and T. Noda, to be published.
16. K. Furuya, M. Piao, N. Ishikawa and T. Saito, Mat. Res. Soc. Symp. Proc. **439**, 331-336 (1997).
17. J. F. Ziegler, J. P. Biersack and U. Littmark, "The stopping and range of ions in solids", Ed. by J. F. Ziegler, Pergaman Press, New York, (1985).
18. E. Abe and M. Nakamura, Phil. Mag. Lett. **75,** 65-73 (1997).
19. X. D. Zhang and M. H. Loretto, Phil. Mag. Lett. **68**, 289-296 (1993).
20. X. D. Zhang and M. H. Loretto, Phil. Mag. A **71**, 421-429 (1995).

(Received December 16, 1999; Accepted May 6, 2000)